Effect of substrate material on phase evolution in reactively sputtered Cr-Al-N films

Y. SUN*, Y. H. WANG, H. P. SEOW
School of Materials Engineering, Nanyang Technological University, Singapore 639798
E-mail: asysun@ntu.edu.sg

Transition metal nitrides such as TiN, CrN and HfN, which normally have the NaCl (B1) type lattice structure, possess excellent mechanical and chemical properties which make them suitable for applications as wear resistant, corrosion resistant, and diffusion barrier coatings. It has been shown that the hardness and the oxidation resistance quality of these nitride coatings can be improved by adding a third element such as aluminum [1–3]. Since aluminum also forms its own nitride, AlN, which normally has the Wurtzite (B4) type lattice structure, the incorporation of Al or AlN in the B1-type nitride coatings will lead to phase transition from B1 to B4 if the solubility limit of AlN in the B1 phase is exceeded [4, 5]. In many cases, nitride films with B4-type structure are not desired due to the low hardness and poor ductility associated with the hexagonal structure. Many studies have thus been conducted on the B1-B4 phase transition, particularly in the Ti-Al-N and Cr-Al-N systems [4–7].

It has been shown that among transition metal nitrides with the B1 structure, CrN has the highest solubility limit for aluminum nitride (AlN) [4]. Theoretical calculation predicted that the solubility limit of AlN in B1 CrN is about 77%, above which the transition from B1 to B4 structure occurs [5]. Since Al has a smaller atomic radius than Cr, the dissolution of AlN in CrN will lead to contraction of the lattice of the cubic B1 structure from that of pure CrN towards that of metastable cubic AlN. Fig. 1 schematically shows the variation of the lattice parameter of the B1 CrAlN phase with AlN content and the transition from B1 to B4. This prediction has been observed by experimental work on co-sputtered Cr-Al-N films on both heated and unheated substrates [4, 5, 8–11]. This has significant implications that the high temperature oxidation resistance of CrN films can be much improved by adding a large amount of aluminum without altering the B1 structure [12].

In the present work, attempts have been made to deposit Cr-Al-N films with Al contents within the solubility limit in B1 structure onto several substrate materials. It was found that the substrate material has a strong influence on the phase constituents in the films. Deviation from theoretical prediction and previous experimental results was observed.

The substrate materials used are polished (100) silicon wafer, commercial aluminum alloy AA6061, and M42 high speed steel (HSS). A planar magnetron sputtering system was used for film deposition. Two sputtering power supplies are available in the system: one is in direct current (DC) mode and the other in radio frequency (RF) mode with an impedance-matching network for the optimization of the RF power input. Cr-Al-N films were fabricated by co-sputtering of the chromium target and the aluminum target in an argon/nitrogen gas mixture with argon to nitrogen flow rate ratio 1:1. The size of the targets is 75 mm in diameter and 5 mm in thickness. The chromium target was sputtered in DC mode, while the aluminum target was sputtered in RF mode, due to the formation of an insulating AlN layer at the target surface. During deposition, the substrate temperature was kept constant at 300 °C and the working pressure was 0.67 Pa. The sputtering power (DC) of the chromium target was kept constant at 250 W, while the sputtering power (RF) of the aluminum target was varied from 50 to 300 W for different depositions. This allowed for the variation of aluminum content in the resultant Cr-Al-N films. A Rigaku Dmax 2200 X-ray diffraction (XRD) instrument with Cu K_α radiation ($\lambda = 0.15406$ nm) was used for XRD measurement to determine the phase constituents in the films. Grazing angle incidence scan with a fixed incidence angle of 2 ° was used. Electron probe microanalysis (EPMA) attached to a scanning electron microscope was performed to measure the chemical compositions of all the films.

Fig. 2 shows the chemical composition of the Cr-Al-N films as a function of aluminum target power. It can be seen that although the chemical composition of the films is slightly dependent on substrate material, at a constant chromium target power (250 W), the aluminum content increases linearly and the chromium content decreases linearly with increasing aluminum target power, while the nitrogen content remains nearly constant at about 50% for all the films. This suggests that the films produced are nearly stoichiometric (Cr:Al)N. From the chemical composition analysis (Fig. 2), it can also be derived that the AlN concentration in all the films produced is less than 35%, which is within the solubility limit of AlN in CrN, as discussed previously.

It is thus expected that all the films produced should have a single B1 CrAlN phase structure, with all the AlN dissolved in CrN. This is indeed the case for the films deposited on the (100) Si substrates, as can be seen

*Author to whom all correspondence should be addressed.

0022–2461

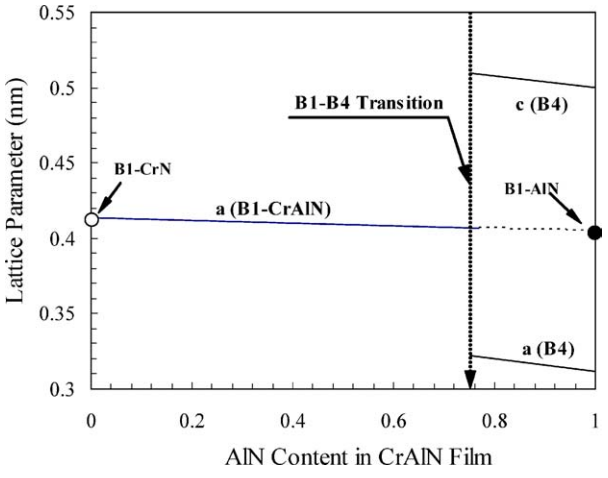

Figure 1 Schematic diagram showing the lattice parameter of CrAlN phase and B1-B4 transition as a function of AlN content in the film.

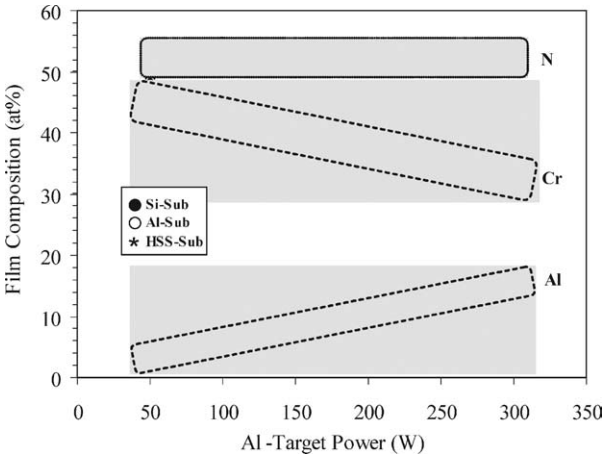

Figure 2 Film composition as a function of aluminum target power for the Cr-Al-N films deposited on the three substrate materials. Constant chromium target power: 250 W.

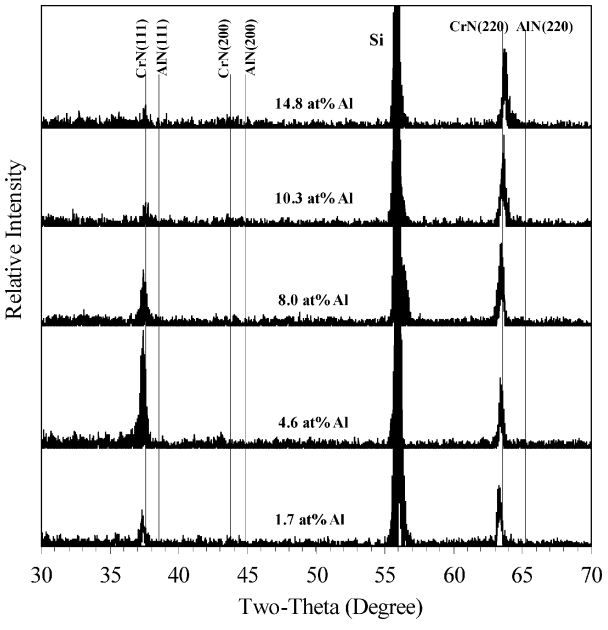

Figure 3 XRD patterns from the Cr-Al-N films with varying amounts of aluminum deposited on (100) Si substrates.

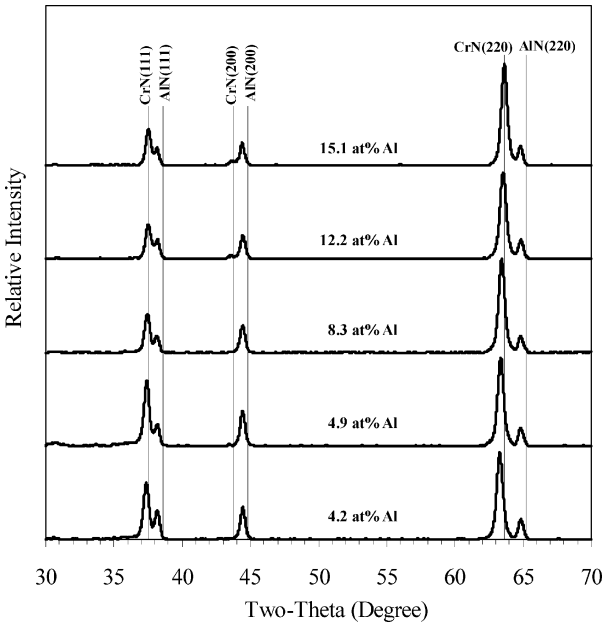

Figure 4 XRD patterns from the Cr-Al-N films with varying amounts of aluminum deposited on aluminum alloy substrates.

from the XRD patterns (Fig. 3). Two diffraction peaks corresponding to B1 CrAlN were detected from each film on (100) Si, with the peak positions being shifted to higher 2θ angles with increasing aluminum content in the film, i.e., the average lattice parameter calculated from the CrAlN (111) and (220) peaks decreases with increasing aluminum content, as can be clearly seen in Fig. 6.

However, each XRD pattern generated from the films deposited on the aluminum alloy substrates is split into two sets of fcc patterns, one corresponding to CrN and the other to metastable cubic AlN (Fig. 4). The peaks from B1 CrN are shifted to higher 2θ angles with increasing aluminum content in the film, indicating the dissolution of some AlN in the B1 CrN lattice. While all the peaks from cubic AlN are shifted to lower 2θ angles, which suggests that some CrN is dissolved in the metastable B1 AlN, causing lattice expansion. Fig. 6 also shows the variation of lattice parameters of the two cubic phases with aluminum content in the film. The lattice parameter of the cubic CrN phase decreases with increasing Al content, suggesting an increasing amount of AlN dissolved in CrN, while the lattice parameter of the AlN phase remains nearly constant in all the films, suggesting that the amount of CrN dissolved in cubic AlN is similar in all the films. The formation of a separate cubic AlN phase in the films also means that the amount of AlN dissolved in the cubic CrN is less than that in the films deposited on (100) Si substrates. This explains the observed larger lattice parameter of the CrN phase on aluminum alloy substrates (Fig. 6). It is also noted that the lattice parameter of the CrN phase on both silicon and aluminum alloy substrates decreases at a similar rate with increasing aluminum content in the film.

For the films deposited on the HSS substrates, in addition to the CrN(111) and CrN(220) peaks, a relatively broad peak positioning at 2θ angle between that for CrN(200) and cubic AlN(200) was detected, while the cubic AlN(111) and (220) peaks were not

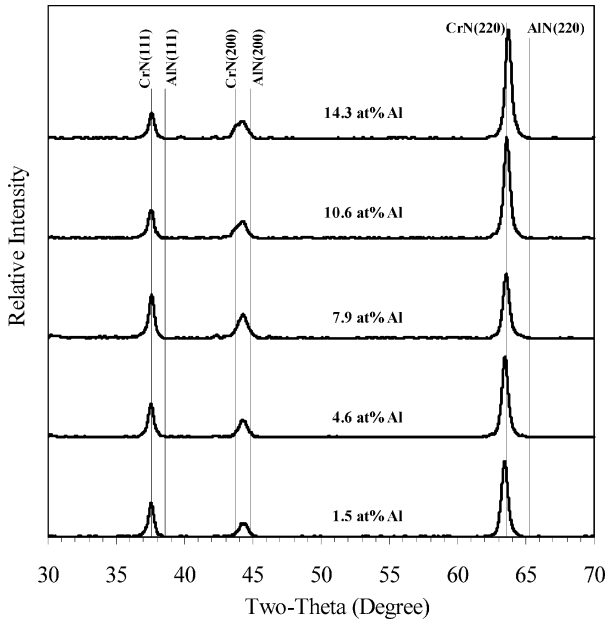

Figure 5 XRD patterns from the Cr-Al-N films with varying amounts of aluminum deposited on high speed steel substrates.

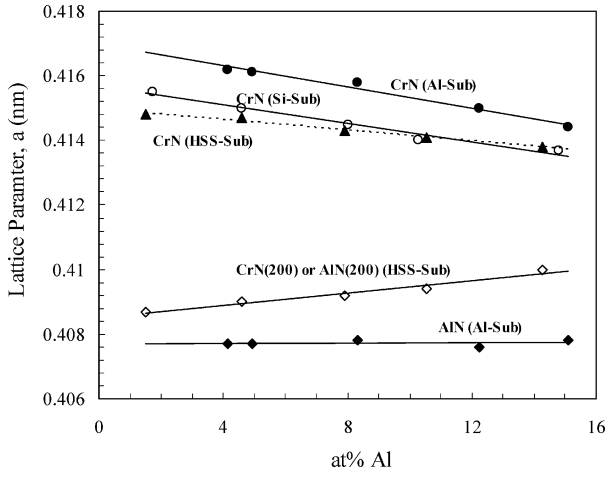

Figure 6 Variation of lattice parameter of B1-CrN and B1-AlN with aluminum content in the Cr-Al-N film.

detected (Fig. 5). The average lattice parameter of the CrN phase calculated from the (111) and (220) peaks also decreases with increasing aluminum content in the film, but at a slower rate than that found for the films deposited on silicon and aluminum alloy substrates (Fig. 6). It thus seems that the aluminum atoms (cations) mainly cluster at the {200} planes of the cubic CrN lattice, causing the large contraction in interplanar spacing along the {200} planes, while in the {111} and {220} planes, the interplanar spacings are less affected by aluminum dissolution.

In summary, substrate material influences phase evolution in reactively co-sputtered Cr-Al-N films with Al contents favorable for B1 phase formation. The films deposited on (100) Si substrates coincide with theoretical prediction and previously experimental results in that a single B1 phase (CrAl)N is evolved. However, two B1 phases, i.e., cubic CrN and cubic AlN, evolve in the films deposited on aluminum alloy substrates, with dissolution of Al in CrN and Cr in AlN. In the films deposited on the HSS substrates, clustering of Al cations at the B1 CrN {200} planes seems to occur, which leads to the large contraction of interplanar spacing along the {200} planes.

References

1. M. A. BAKER, C. REBHOLZ, A. LEYLAND and A. MATTHEWS, *Vacuum* **67** (2002) 471.
2. T. IKEDA and H. SATOH, *Thin Solid Films* **195** (1991) 99.
3. K. YAMAMOTO, T. SATO, K. TAKAHARA and K. HANAGURI, *Surf. Coat. Tech.* **174/175** (2003) 620.
4. A. SUGISHIMA, H. KAJIOKA and Y. MAKINO, *ibid.* **97** (1997) 590.
5. Y. MAKINO and K. NOGI, *ibid.* **98** (1998) 1008.
6. T. LEYENDECKER, O. LEMMER, S. ESSER and J. EBBERINK, *ibid.* **48** (1991) 175.
7. B.-Y. SHEW, J.-L. HUANG and D.-F. LII, *Thin Solid Films* **293** (1997) 212.
8. J. VETTER, E. LUGSCHEIDER and S. S. GUERREIRO, *Surf. Coat. Tech.* **98** (1998) 1233.
9. S. ULRICH, H. HOLLECK, J. YE, H. LEISTE, R. LOOS, M. STUBER, P. PESCH and S. SATTEL, *Thin Solid Films* **437** (2003) 164.
10. E. LUGSCHEIDER, K. BOBZIN, TH. HORING and M. MAES, *ibid.* **420/421** (2002) 318.
11. M. HIRAI, T. SUZUKI, H. SUEMATSU, W. JIANG and K. YATSUI, *J. Vac. Sci. Technil.* A **21** (2003) 947.
12. M. HIRAI, H. SAITO, T. SUZUKI, H. SUEMATSU, W. JIANG and K. YATSUI, *Thin Solid Films* **407** (2002) 122.

Received 21 March
and accepted 3 June 2004